PERGAMON

Electrochimica Acta 48 (2002) 241–246

ELECTROCHIMICA Acta

www.elsevier.com/locate/electacta

Low temperature performance of graphite electrode in Li-ion cells

S.S. Zhang *, K. Xu, T.R. Jow

U.S. Army Research Laboratory, Sensors and Electron Devices Directorate, Adelphi, MD 20783, USA

Received 12 April 2002; received in revised form 21 August 2002

Abstract

We studied low temperature performance of Li/graphite cell. Results show that capacity of the graphite electrode falls significantly in the temperature range of 0 to −20 °C. When lithiation and delithiation are both carried out at −20 °C, graphite only retains 12% of the room temperature capacity. However, delithiation capacity of graphite increases to 92% of the room temperature value if the lithiation is carried out at room temperature. We believe that the poor low temperature performance of the cell is due to slow kinetics of lithium ion diffusion in graphite rather than low ionic conductivity of electrolyte and solid electrolyte interface (SEI) on the graphite surface. During lithiation and delithiation processes, lithium ion has the similar apparent chemical diffusion coefficient of 10^{-9}–10^{-10} cm^2/s at 20 °C, depending on the state of lithiation of graphite. We observed a dramatic decrease in lithium ion diffusivity in the temperature range of 0 to −20 °C, and that at low temperatures of < −20 °C, lithium ion has higher diffusivity in the delithiated graphite than in the lithiated one. We also observed that temperature dependence of cycling behavior of the Li/graphite cell follows the change of lithium ion diffusivity.

Keywords: Li-ion cell; Graphite electrode; Low temperature; Lithium ion diffusivity; Ionic conductivity

1. Introduction

Many papers have addressed the issue about poor low temperature performance of Li-ion cells [1–12]. A common phenomenon is that the Li-ion cell loses most of its capacity and power as the temperature falls below −10 °C. Plichta and Behl reported that at −40 °C the capacity of Li-ion cell only retained 12% of the room temperature capacity [1]. Similar results also have been reported by other researchers [3,7,8]. For this problem, early understanding was based on the low ionic conductivity of electrolyte and solid electrolyte interface (SEI) on the graphite surface. Therefore, previous solutions were mainly focused on development of the liquid electrolytes that have low freezing point and high ionic conductivity [2,4,5,9,10]. In many cases, this approach indeed led to an improved low temperature performance. However, recent studies revealed that the ionic conductivity of the electrolytes is not the key factor to limit low temperature operation of the Li-ion cells [3,6,7,11,12], and that the main limitation arises from the graphite anode instead of the cathode [3,6,7]. For these findings, Huang et al. [3] proposed that the real limitation is the low diffusivity of lithium ion in graphite. This hypothesis has been further explained in the term of electric polarization of the graphite electrode, which is caused by the low diffusivity of lithium ion [6,7]. In this work, we attempt to confirm above proposal by directly measuring chemical diffusion coefficient of lithium ion and observing its temperature dependence in the low temperature range.

Several electrochemical techniques have been developed to determine chemical diffusion coefficient (D) of lithium ion in carbons, such as electrochemical impedance spectroscopy (EIS) [13], slow scan cyclic voltammetry [14], potential intermittent titration technique [15], potential relaxation technique [16], current pulse relation [17], and potential step chronoamperometry (PSCA) [17–19]. The reported D values of lithium ion in various carbons using these techniques vary greatly from 10^{-8} to 10^{-11} cm^2/s [13]. In the present work, we selected PSCA method to measure the apparent D of lithium ion in natural graphite. Correlation of lithium

* Corresponding author. Tel.: +1-301-394-0981; fax: +1-301-394-0273

E-mail address: szhang@arl.army.mil (S.S. Zhang).

0013-4686/02/$ - see front matter
PII: S0013-4686(02)00620-5

ion diffusivity and low temperature performance of the graphite electrode will be discussed.

2. Experimental

Natural graphite (99+%, with an average particle size of 18 μm and a product code number of LF-18A) was purchased from International Technology Exchange Society (ITE). Graphite powder was coated onto a copper foil using 5 wt.% of poly(vinylidene difluoride) (PVDF) as binder. Electrolyte used in this work was a 1 m (mole salt per kilogram solvent) $LiPF_6$ dissolved in a 3:7 (wt.) mixture of ethylene carbonate (EC) and ethyl methyl carbonate (EMC), which was prepared in an argon-filled glove-box and determined to have 10–15 ppm of water content by Karl–Fischer titration. Li/graphite button cells with a graphite electrode area of 1.27 cm^2 were assembled in the same glove-box with both oxygen and water contents less than 20 ppm. A Tenney Environmental Oven Series 942 was used to provide a constant temperature environment for the test. The cell was cycled using a Maccor Series 4000 tester at a current density of 0.1 mA/cm^2 between 0.002 and 1.0 V.

Solartron SI 1287 Electrochemical Interface and SI 1260 Impedance/Gain-Phase Analyzer, controlled by a personal computer using CorrWare and Zplot softwares, were employed to make measurements of EIS and PSCA. Ac impedance of the cell was potentiostatically measured by applying a dc bias equal to the cell's open circuit voltage and an ac oscillation of 5 mV amplitude over the frequencies from 100 kHz to 0.001 Hz. The obtained EIS data were analyzed by using ZView software (Scribner and Associates, Inc.). PSCA measurement was carried out by applying a potential step of every 10 mV. Each potential step was last for 10 h or until the current fell to below 5 μA, whichever came first. Slow scan rate cyclic voltammetry of the cell was performed at 0.001 mV/s using an EG&G PAR Potentiostat/Galvanostat Model 273A.

3. Results and discussion

3.1. Cycling behavior at room temperature

It is known that graphite electrode undergoes a SEI formation on its surface during the initial few cycles [20,21], which usually develops some irreversible capacities. To reduce the complication that may arise from the initial irreversible capacities, we cycled the cell for 10 times before the measurements were made. Fig. 1 shows voltage of the Li/graphite cell as a function of capacity, which was obtained from the 11th cycle at 0.1 mA/cm^2. Three voltage plateaus in Fig. 1 indicate a typically

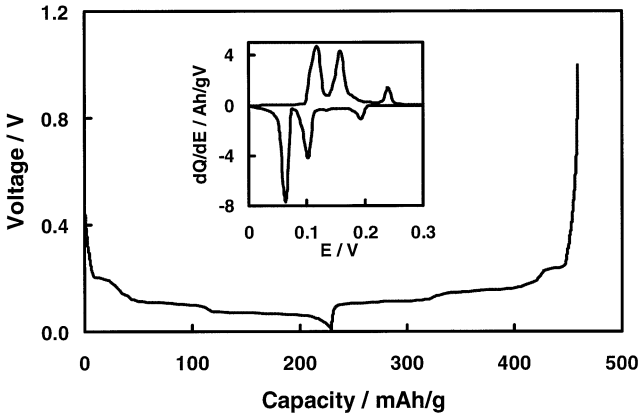

Fig. 1. Voltage–capacity curve of Li/graphite cell at room temperature, which was recorded from the 11th cycle at 0.1 mA/cm^2. Inset shows differential capacity–voltage plot of the cell.

electrochemical process of the graphite electrode with lithium ion [20–22], which can be better displayed by three distinct peaks in the differential capacity–voltage plot (inset). Levi et al. [21] reported that these three peaks, respectively correspond to the following electrochemical processes (phase–phase transitions) of the graphite electrode: $LiC_{72}+Li \Leftrightarrow 2LiC_{36}$, $4LiC_{27}+5Li \Leftrightarrow 9LiC_{12}$, and $LiC_{12}+Li \Leftrightarrow 2LiC_6$. Inset of Fig. 1 exhibits that the lithiation process always carries a low differential capacity plateau in the voltage region of 0.2–0.1 V. This characteristic is known to be ascribed to the transition of $3LiC_{36}+Li \Leftrightarrow 4LiC_{27}$ between the 1st and 2nd transitions [21]. Coulombic efficiency of the delithiation process in Fig. 1 is calculated to be nearly 100%.

3.2. Capacity change with temperature

After cycled at room temperature, the Li/graphite cell was tested at different temperatures, respectively. In a separate experiment, we found that the temperature equilibrium time between 2 h and 10 days made a negligible difference in the cell performance. Therefore, a minimum time of 2 h was taken to equilibrate the temperature before the cycling test was carried out. A 24-h rest at the open circuit was provided between lithiation and delithiation of the cell. Fig. 2 plots cycling performance of the cell at various temperatures, which was obtained by discharging and charging the cell at the same temperature and current density (0.1 mA/cm^2). One may find from Fig. 2 that, with lowering of the temperature, charge (delithiation) capacity of the Li/graphite cell decreases and electric polarization increases as indicated by the potentials at which delithiation takes place. In particular, a significant change in the capacity (decrease) and polarization voltage (increase) is observed in the temperature range from −10 to −20 °C. At −20 °C, the cell only retains 12% of the capacity

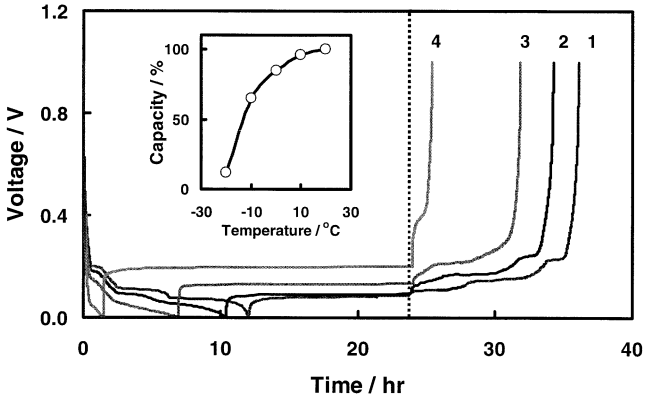

Fig. 2. Cycling performance of Li/graphite cell at various temperatures, which was obtained by discharging and charging the cell at the same temperature and current density (0.1 mA/cm^2). In order to plot all charge processes at the same starting point, the cell was taken a rest at open circuit for a different time between the charge and discharge experiments, as shown by a voltage plateau. Inset shows relative charge (delithiation) capacity of the cell versus the capacity obtained at 20 °C. (1) 20, (2) 0, (3) −10, and (4) −20 °C.

obtained at 20 °C (inset in Fig. 2). This observation is similar to those reported elsewhere [1,3,7,8].

To understand the origin for this dramatic change of the capacity and polarization at the temperatures between −10 and −20 °C, we measured and analyzed EIS data of the Li/graphite cell at various temperatures. All EISs of the cell were recorded from a charged (delithiated) state. Typically, EIS of the cell consists of two overlapped semicircles at high and medium frequency regions, and a slopping straight line at low frequency regions. Fig. 3 exhibits an example of the EIS and an equivalent circuit used to interpret the electrochemical process of lithium ion intercalation into graphite [20,23,24]. R_e presents the resistance of cell bulk including electrolyte, electrode and separator. R_f and C_f are the resistance and capacitance of the SEI, respectively, and R_{ct} and C_{dl} are the charge-transfer resistance and its related double-layer capacitance, respectively. W is the Warburg impedance arising from the semi-infinite diffusion of lithium ion in graphite electrode.

Temperature dependence of the resistances (R_e, R_f, and R_{ct}) of the delithiated Li/graphite cell is plotted in Fig. 4, which indicates such a trend: all three resistances increase with the decrease of temperature. It is shown that, with the temperature falling, the R_e and R_f values are increased at a similar rate, and that the increasing trend is continuous without appearance of an abrupt increase as reflected by a significant decrease in the capacity. This suggests that ionic conductivity of the electrolyte and SEI may not be a main reason for the dramatic drop of cycling performance at the low temperatures. However, the R_{ct} increases much faster than both R_e and R_f, and appears to dominate the total resistance of the Li/graphite cell at the low temperatures (< -20 °C). Thus, it may be concluded that the limitation to the low temperature performance of the Li/graphite cell is the electrochemical kinetics of lithium ion diffusion, because the R_{ct} reflects a transfer process of the lithium ion on the interface between the graphite and electrolyte.

3.3. Effect of lithiation temperature on delithiation capacity

It is known that delithiation capacity of graphite at the low temperatures (< -20 °C) will be substantially increased when the cell is lithiated at room temperature. Fig. 5 compares the voltage–capacity correlation of the charge (delithiation) process at different temperatures for the Li/graphite cell that was first discharged (lithiated) to 0.002 V at 0.1 mA/cm^2 at 20 °C. As a result, the present cases show much higher capacity at the low temperatures. Delithiation capacity of graphite

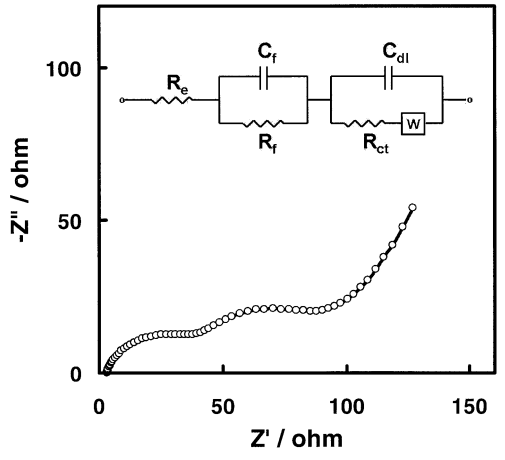

Fig. 3. Typical EIS of Li/graphite cell and an equivalent circuit used for analysis of the electrochemical process of lithium ion in graphite.

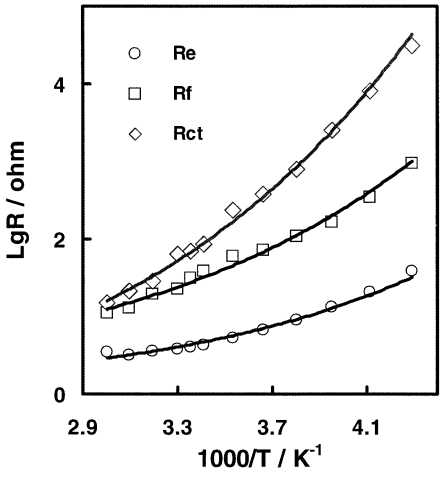

Fig. 4. Temperature dependence of the resistance of cell bulk (R_e), SEI (R_f), and charge-transfer (R_{ct}), respectively.

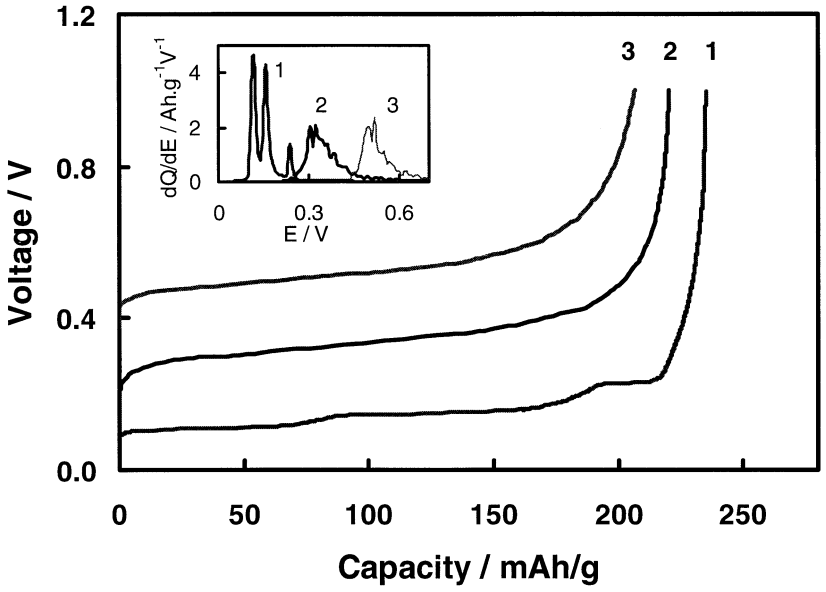

Fig. 5. Voltage–capacity curve of charge (delithiation) process for Li/graphite cell, which was obtained by discharging the cell at 20 °C and charging at a specified temperature. Inset shows differential capacity–voltage plot of delithiation process. Current density was 0.1 mA/cm^2. (1) 20, (2) −20, and (3) −30 °C.

is increased to 94% at −20 °C and 88% at −30 °C, respectively, in comparison to that obtained at 20 °C. Relatively lower capacity here may be ascribed to the decrease in ionic conductivity of the electrolyte and SEI at the low temperatures. Fig. 5 displays that the cell has about 0.20 V higher polarization voltage at −20 °C than at 20 °C, which corresponds to a positive shift (∼0.20 V) of the peak potentials in the differential capacity (see inset).

To account for the difference in cycling performance of the lithiated and delithiated graphite, we analyzed EIS data of these two states. EISs of the Li/graphite cell at low temperatures for the lithiated and delithiated states, respectively, are presented in Fig. 6, in which the inset is a blowup of the high frequency regions. It is seen from inset of Fig. 6 that the lithiated and delithiated states have the same R_e and R_f values. The only difference that we could notice in Fig. 6 is the R_{ct} value. That is, the delithiated state has larger R_{ct} value than the lithiated state. This result explains the fact that, at the low temperatures, lithiation into delithiated graphite is more difficult than delithiation out of lithiated graphite.

3.4. Diffusivity of lithium ion in graphite

In order to understand low temperature performance of the Li/graphite cell, we measured chemical diffusion coefficient (D) of the lithium ion in graphite. Apparent D of lithium ion in graphite may be calculated from PSCA data of the Li/graphite cell [17–19]. A linear correlation of the $\ln|I|$–t plot generally exists in a certain time region. We may calculate the D value from PSCA by assuming the following conditions: (1) the current is controlled by diffusion of lithium ion in graphite; and (2) the particle of graphite is spherical and the diffusion length is the apparent radius of the particle. Thus, the D may be calculated from the slope of Lg$|I|$–t plot that is expressed by Eq. (1) for the time domain $t > a^2/\pi^2 D$ [17–19]:

$$I = (2nFA\Delta C/a)\exp[(-\pi^2 D/a^2)t] \quad (1)$$

where F is Faraday constant, A is the surface area of graphite electrode, ΔC is the variation of lithium concentration in the particle during the potential step, and a is the radius of the particle.

Fig. 7 plots Lg D of lithium ion as a function of the potential (E) of graphite. For comparison, a slow scan rate cyclic voltammogram (CV) of the Li/graphite cell is also illustrated in Fig. 7. Obviously, there are four minima of the D values for both lithiation and delithiation processes, which well correspond to those of the CV peaks (see their correspondent correlation of the peaks marked by letters a, b, c, d, a′, b′, c′ and d′). Similar results about this peak-shape Lg D–E correlation have been reported by other researchers [16,17,19,25]. It is known that multiple phase–phase transitions of lithium graphite insertion compounds take place in peak potential regions of the CV, where generally exists a high energy barrier for lithium ion migration [21]. This could be the origin for the appearance of four minima of the D values in the potential range of 0–0.3 V. Fig. 7 displays that in the studied voltage range the D of lithium ion in graphite is 10^{-9}–10^{-10} cm^2/s at 20 °C. This value is in the similar order of magnitude as those reported elsewhere [13,16,19,25,26]. In order to observe the correlation between the diffusivity of lithium ion and

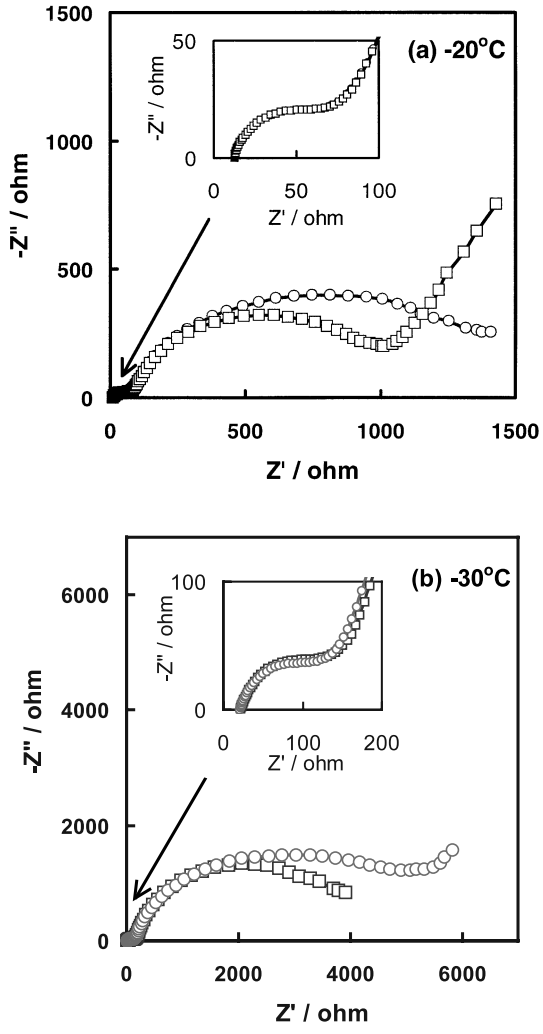

Fig. 6. Comparison for EISs of Li/graphite cell at fully lithiated (squares) and delithiated (circles) states. Inset shows an enlarged part in the high frequency regions. (a) −20 and (b) −30 °C.

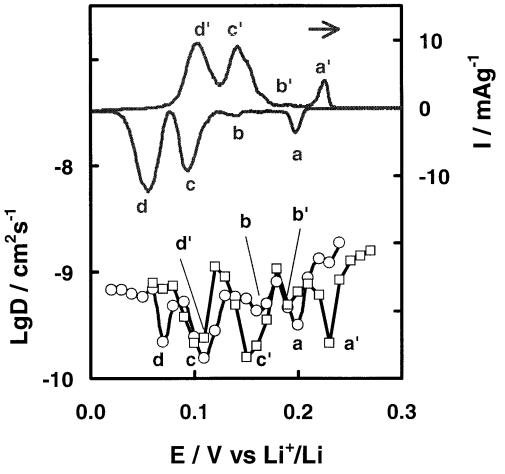

Fig. 7. The top is a slow scan rate cyclic voltammogram of Li/graphite cell at 0.001 mV/s; The bottom shows potential dependence of lithium ion diffusivity at 20 °C for lithiation (circles) and delithiation (squares) processes, respectively.

the composition (potential status) of lithium graphite insertion compound, we plot both the lithium ion diffusivity and the cell voltage versus graphite capacity in Fig. 8, which again exhibits four minima of the D values with the same reason as described in Fig. 7. It is observed from Fig. 8 that, in most of capacity regions, the lithiation and delithiation processes have nearly the same diffusivity of lithium ion although several researchers reported that lithium ion has higher diffusivity during delithiation than during lithiation [16,26]. This result accords with the fact that the Li/graphite cell shows nearly the same performance in both lithiation and delithiation processes when the cell is cycled around room temperature.

Effect of the temperature on the D value of lithium ion in the lithiated and delithiated graphite, respectively, is illustrated in Fig. 9, from which we find that these two states have the similar diffusivity as the temperature is above 0 °C. A dramatic decrease in the D value occurs in the temperature range of 0 to −20 °C. This result is in accordance with the facts that the cell performance drops abruptly and the R_{ct} increases sharply at the temperatures of lower than 0 °C. When the temperature falls to −20 °C or lower, diffusivity of lithium ion in the delithiated graphite becomes lower than that in the lithiated one. This implies that electrochemical kinetics of the lithium ion diffusion in the delithiated graphite is slower than in the lithiated one. In other words, at the low temperatures lithiation (discharge) of a Li/graphite cell from a delithiated state is more difficult than the reverse (delithiation) process. It may be concluded from the above discussion that difference in the electrochemical kinetics of lithium ion diffusion in graphite is the

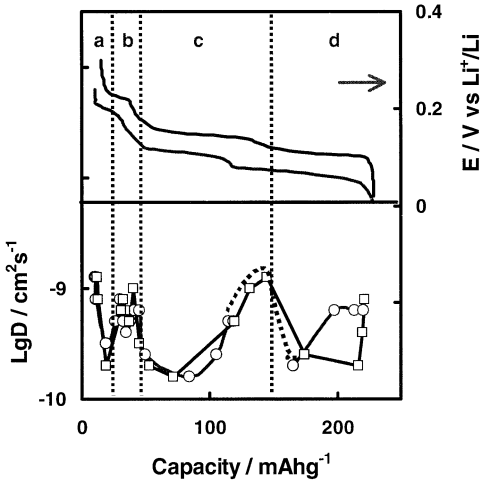

Fig. 8. The top is a voltage–capacity plot of the lithiation and delithiation processes, respectively, which was obtained at 0.1 mA/cm^2. The bottom shows capacity (i.e. state of lithiation or composition of Li_xC_6) dependence of lithium ion diffusivity at 20 °C for the lithiation (circles) and delithiation (squares) processes, respectively. Note that two diffusivity data in lithiation process were missed, as shown by a dotted line.

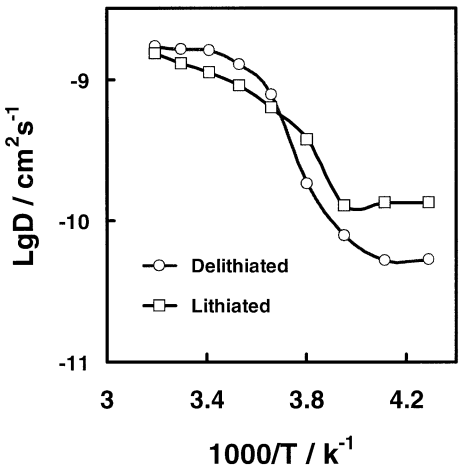

Fig. 9. Lg D of lithium ion in graphite as a function of $1/T$ for the lithiated (squares) and delithiated (circles) graphite, respectively.

main reason for the asymmetrical capacity between the lithiation and delithiation processes at the low temperatures.

4. Conclusion

Cycling performance of Li/graphite cell is affected by many factors such as ionic conductivity of the electrolyte and SEI on the graphite surface, diffusivity of lithium ion in graphite. When the temperature falls from 0 to −20 °C, capacity of the Li/graphite cell is dramatically reduced, which is accompanied by a significant increase in charge-transfer resistance of the cell. This fact indicates that poor low temperature performance of graphite mainly originates from the slow kinetics of lithium ion diffusion in graphite. On the other hand, the lithiation temperature has a profound impact on the delithiation capacity at the temperatures of below −20 °C. At −20 °C, graphite only retains 12% of its room temperature delithiation capacity when lithiated at −20 °C, while 94% can be retained once lithiated at room temperature. This discrepancy in temperature dependence of the capacity is in well accordance with the asymmetry of lithium ion diffusivity in graphite at low temperatures. When the temperature is above 0 °C, lithium ion has the similar diffusivity (in the range of 10^{-9}–10^{-10} cm^2/s at 20 °C) in both lithiated and delithiated graphite. However, in the temperature range of below 0 °C, lithium ion diffusivity in the delithiated graphite becomes increasingly lower than that in the lithiated graphite with the temperature decreasing.

References

[1] E.J. Plichta, W.K. Behl, Proceedings of the 38th Power Sources Conference, Cherry Hill, NJ, 8–11 June, 1988, p. 444.
[2] M.C. Smart, B.V. Ratnakumar, S. Surampudi, J. Electrochem. Soc. 146 (1999) 486.
[3] C.K. Huang, J.S. Sakamoto, J. Wolfenstine, S. Surampudi, J. Electrochem. Soc. 147 (2000) 2893.
[4] H.C. Shiao, D. Chua, H.P. Lin, S. Slane, M. Salomon, J. Power Sources 87 (2000) 167.
[5] E.J. Plichta, W.K. Behl, J. Power Sources 88 (2000) 192.
[6] M. Salomon, H.P. Lin, D. Chua, A. Shiao, F. Cassel, V. Manivannan, S. Bansal, High Power Electrochemical Sources Workshop, Rethymnon, Crete, 2–5 October, 2000.
[7] H.P. Lin, D. Chua, M. Salomon, H.C. Shiao, M. Hendrickson, E. Plichta, S. Slane, Electrochem. Solid-State Lett. 4 (2001) A71.
[8] G. Nagasubramanian, J. Appl. Electrochem. 31 (2001) 99.
[9] E.J. Plichta, M. Hendrickson, R. Thompson, G. Au, W.K. Behl, M.C. Smart, B.V. Ratnakumar, S. Surampudi, J. Power Sources 94 (2001) 160.
[10] S. Herreyre, O. Huchet, S. Barusseau, F. Perton, J.M. Bodet, P. Biensan, J. Power Sources 97–98 (2001) 576.
[11] S.S. Zhang, K. Xu, T.R. Jow, J. Solid State Electrochem., in press.
[12] S.S. Zhang, K. Xu, J.L. Allen, T.R. Jow, J. Power Sources 110 (2002) 217.
[13] P. Yu, B.N. Popov, J.A. Ritter, R.E. White, J. Electrochem. Soc. 146 (1999) 8.
[14] M.D. Levi, D. Aurbach, J. Electroanal. Chem. 421 (1997) 89.
[15] M.D. Levi, D. Aurbach, J. Phys. Chem. B 101 (1997) 4641.
[16] Q. Wng, H. Li, X. Huang, L. Chen, J. Electrochem. Soc. 148 (2001) A737.
[17] T. Uchida, Y. Morikawa, H. Ikuta, M. Wakihara, K. Suzuki, J. Electrochem. Soc. 143 (1996) 2606.
[18] H. Ura, T. Nishina, I. Uchida, J. Electroanal. Chem. 369 (1995) 169.
[19] M. Nishizawa, R. Hashitani, T. Itoh, T. Matsue, I. Uchida, Electrochem. Solid-State Lett. 1 (1988) 10.
[20] S.S. Zhang, M.S. Ding, K. Xu, J. Allen, T.R. Jow, Electrochem. Solid-State Lett. 4 (2001) A206.
[21] T. Ohzuku, Y. Iwakoshi, K. Sawai, J. Electrochem. Soc. 140 (1993) 2496.
[22] M.D. Levi, D. Aurbach, J. Electroanal. Chem. 421 (1997) 79.
[23] T. Piao, S.M. Park, C.H. Doh, S.I. Moon, J. Electrochem. Soc. 146 (1999) 2794.
[24] Y.C. Chang, J.H. Jong, G.T. Fey, J. Electrochem. Soc. 147 (2000) 2033.
[25] D. Aurbach, M.D. Levi, E. Levi, H. Teller, B. Markovsky, G. Salita, J. Electrochem. Soc. 145 (1988) 3024.
[26] J.S. Gnanaraj, M.D. Levi, E. Levi, G. Salitra, D. Aurbach, J.E. Fischer, A. Claye, J. Electrochem. Soc. 148 (2001) A525.